

Determining Amyloid- β positivity using [^{18}F]AZD4694 PET imaging

Joseph Therriault BSc^{1,2,3}, Andrea L. Benedet PhD^{1,2,3}, Tharick A. Pascoal MD,PhD^{1,2,3}, Melissa Savard MSc¹, Nicholas J. Ashton PhD^{4,5}, Mira Chamoun PhD^{1,2}, Cecile Tissot BSc^{1,2,3}, Firoza Lussier BSc^{1,2,3}, Min Su Kang BSc^{1,2,3}, Gleb Bezgin PhD^{1,2,3}, Tina Wang MSc^{1,2,3}, Jaime Fernandes-Arias MSc^{1,2,3}, Gassan Massarweh PhD^{3,6}, Paolo Vitali MD,PhD², Henrik Zetterberg MD,PhD^{4,5}, Kaj Blennow MD,PhD^{4,5}, Paramita Saha-Chaudhuri PhD⁷, Jean-Paul Soucy MD MSc^{2,3}, Serge Gauthier MD,FRCPC^{1,2}, and Pedro Rosa-Neto MD,PhD^{1,2,3}

¹Translational Neuroimaging Laboratory, The McGill University Research Centre for Studies in Aging, Douglas Hospital, McGill University, Montreal, Canada.

²Department of Neurology and Neurosurgery, McGill University, Montreal, Canada.

³Montreal Neurological Institute, Montreal, Canada.

⁴Department of Psychiatry and Neurochemistry, Institute of Neuroscience and Physiology, University of Gothenburg, Mölndal, Sweden

⁵Clinical Neurochemistry Laboratory, Sahlgrenska University Hospital, Mölndal, Sweden

⁶Department of Radiochemistry, McGill University, Montreal, Canada

⁷Department of Epidemiology and Biostatistics, McGill University, Montreal, Canada

Keywords: Alzheimer's disease, Amyloid- β , Positron Emission Tomography, 18F-AZD4694

Running title: Amyloid- β positivity with 18F-AZD4694

Submission Type:**Original Article**

Number of characters in Title:**63**

Number of Tables:**1**

Number of figures:**5**

Word count of abstract: 335

Word count of Paper: 2433

Immediate Open Access: Creative Commons Attribution 4.0 International License (CC BY) allows users to share and adapt with attribution, excluding materials credited to previous publications.

License: <https://creativecommons.org/licenses/by/4.0/>.

Details: <http://jnm.snmjournals.org/site/misc/permission.xhtml>.



ABSTRACT

Amyloid- β deposition into plaques is a pathological hallmark of Alzheimer's disease (AD) appearing years before the onset of symptoms. Although cerebral amyloid- β deposition occurs on a continuum, dichotomization into positive and negative groups has advantages for diagnosis, clinical management and population enrichment for clinical trials. 18F-AZD4694 (also known as 18F-NAV4694) is an amyloid- β imaging ligand with high affinity for amyloid- β plaques. Despite being employed in multiple academic centers, no studies have assessed a quantitative cut-off for amyloid- β positivity using 18F-AZD4694 PET. **Methods:** We assessed 176 individuals [young adults ($n = 22$), cognitively unimpaired elderly ($n = 89$), and cognitively impaired ($n = 65$)] who underwent amyloid- β PET with 18F-AZD4694, lumbar puncture, structural MRI, and genotyping for *APOE ϵ 4*. 18F-AZD4694 values were normalized using the cerebellar grey matter as a reference region. We compared five methods for deriving a quantitative threshold for 18F-AZD4694 PET positivity: comparison with young controls SUVRs values, Receiver Operating Characteristic (ROC) curves based on clinical classification of CU elderly vs AD dementia, ROC curves based on visual A β ⁺/A β ⁻ classification, Gaussian Mixture Modeling and comparison with cerebrospinal fluid measures of amyloid- β , specifically the A β ₄₂/A β ₄₀ ratio. **Results:** We observed good convergence between four methods: ROC curves based on visual classification (optimal cut point: 1.55 SUVR), ROC curves based on clinical classification (optimal cut point: 1.56 SUVR) Gaussian Mixture Modeling (optimal cut point: 1.55 SUVR) and comparison with CSF measures of amyloid- β (optimal cut point: 1.51 SUVR). Means and 2 standard deviations from young controls resulted in a lower threshold (1.33 SUVR) that did not agree with the other methods and labeled the majority of elderly individuals as A β ⁺. **Conclusion:** Good convergence was obtained between a number of methods for determining an optimal cut-off for 18F-AZD4694 PET positivity. Despite

conceptual and analytical idiosyncrasies linked with dichotomization of continuous variables, an ^{18}F -AZD4694 threshold of 1.55 SUVR had reliable discriminative accuracy. While clinical use of amyloid-PET currently is made by visual inspection of scans, quantitative thresholds may be helpful to arbitrate disagreement among raters or in borderline cases.

INTRODUCTION:

The advent of amyloid- β imaging using PET (1) and cerebrospinal fluid measurements of amyloid- β (2,3) have revolutionized the field of Alzheimer's disease (AD) research. Longitudinal amyloid-PET imaging studies of autosomal-dominant (4) and sporadic (5) AD provide evidence that amyloid- β pathology accumulates many years before the onset of cognitive symptoms, suggesting that semi-quantification of amyloid- β plaques *in vivo* permits the early identification of Alzheimer's pathological change (6). Although brain amyloid- β deposition occurs on a continuum (7), stratification of populations using amyloid- β levels is critical for diagnosis of AD, assessing clinicopathological changes associated with amyloid- β , and for selecting individuals to test disease-modifying therapies.

With amyloid-PET increasingly incorporated into clinical care (8), recent multicenter studies have provided evidence that amyloid-PET positivity is associated with changes in clinical management of individuals with cognitive impairment (9). Furthermore, amyloid-PET positivity is frequently used as an enrollment criteria for AD clinical trials (10) with continuous measures used to monitor target engagement (11,12). While "visual reading" of amyloid-PET scans is commonly employed in dichotomization of amyloid-PET images (9,13), this method has important limitations (14,15). Defining quantitative thresholds may provide additional information to visual reads which may facilitate classification of visually borderline cases.

18F-AZD4694 is a high affinity [equilibrium dissociation constant (K_d) = 2.3 nM] (16) radioligand for imaging amyloid- β plaques that displays lower white matter binding compared to other fluorinated amyloid-PET tracers (17,18), enabling easier visual reads. 18F-AZD4694 is a

fluorinated amyloid- β imaging compound structurally resembling [^{11}C]PiB (18). It's radioactive half-life of 110 minutes enables centralized production with the potential for widespread clinical use. In this study, we aim to further describe 18F-AZD4694 by determining a quantitative threshold for amyloid- β positivity with 18F-AZD4694 PET using multiple approaches.

MATERIALS AND METHODS:

Participants

We assessed young adults (n=22), cognitively unimpaired elderly (n=89), and cognitively impaired (n=65) subjects who underwent amyloid- β PET with 18F-AZD4694, lumbar puncture, structural MRI, and genotyping for *APOE* ϵ 4. All individuals in this study were part of the Translational Biomarkers in Aging and Dementia (TRIAD) cohort (19), a longitudinal imaging and biofluid cohort study of aging and neurodegenerative diseases. Evaluations of participants included a review of their medical history and an interview with the participant and their study partner, a neurological examination by a physician and a neuropsychological examination. Participants were assigned a diagnosis of cognitively unimpaired (CU; defined as not MCI or AD dementia(20)), MCI (21) or AD dementia(22) using established clinical criteria. Individuals with MCI and AD dementia were classified as having cognitive impairment (CI). Within the CI group, 32 individuals had a diagnosis of MCI and 33 individuals had a diagnosis of AD dementia. All subjects had detailed clinical assessments including neurological and physical evaluation, Mini-Mental State Examination (MMSE), Clinical Dementia Rating (CDR), and cerebrovascular disease risk. This study's protocol was approved by McGill University's Institutional Review Board and informed written consent was obtained from each subject.

CSF assays

CSF amyloid- β concentrations ($A\beta_{40}$ and $A\beta_{42}$) were measured using the fully automated LUMIPULSE® G1200 instrument (Fujirebio, Ghent, Belgium) according to procedures from the manufacturer. LUMIPULSE measured $A\beta_{42}$ and $A\beta_{40}$ using antibody-coated beads for capture and monoclonal antibodies for detection (23). For analyses using CSF measurements, we compared 18F-AZD4694 SUVR with the $A\beta_{42}/A\beta_{40}$ ratio ($A\beta_{42}$ concentrations normalized to concentrations of the 40 amino acid-long form of amyloid- β [$A\beta_{40}$]), as a recent review provides substantial evidence that the $A\beta_{42}/A\beta_{40}$ ratio has superior diagnostic performance (lower false positive and lower false negative rates) (24). Furthermore, the $A\beta_{42}/A\beta_{40}$ ratio displays higher correspondence with amyloid-PET than measures of the $A\beta_{42}$ alone (25). Amyloid- β positivity on CSF was determined based on a published cut-off of a $A\beta_{42}/A\beta_{40}$ ratio of 0.068 from the LUMIPULSE assay (23).

PET image acquisition and processing

Radiosynthesis of 18F-AZD4694 is described in the supplement and represented in Supplemental Fig. 1. PET acquisition and processing has been described previously (19). 18F-AZD4694 images were acquired 40–70 minutes post-injection and scans were reconstructed with the OSEM algorithm on a 4D volume with 3 frames (3x600s). T1-weighted images were acquired on a 3T Siemens Magnetom using a standard head coil. A MPRAGE MRI sequence was employed to obtain a high-resolution T1-weighted anatomical image of the entire brain. T1-weighted images were non-uniformity and field-distortion corrected and processed using an in-house pipeline. Then, PET images were automatically registered to the T1-weighted image space, and the T1-weighted

images were linearly and non-linearly registered to the ADNI template space. The ADNI template space is a stereotaxic template developed based on the brain CU elderly, MCI and AD dementia individuals, and has superior performance for image registration in neuroimaging studies of aging and dementia than the MNI152 template (26). Subsequently, a PET non-linear registration was performed using the linear and non-linear transformations from the T1-weighted image to the ADNI space and the PET to T1-weighted image registration. The PET images were spatially smoothed to achieve a final resolution of 8mm full-width at half maximum. All images were visually inspected to ensure proper alignment to the ADNI template. 18F-AZD4694 SUVR maps were generated using the cerebellar grey matter as a reference region. Partial volume correction (PVC) was carried out using methods described in (19); all analyses were repeated using PVC data.

A global 18F-AZD4694 SUVR value was estimated for each participant by averaging the SUVR from the precuneus, prefrontal, orbitofrontal, parietal, temporal, anterior, and posterior cingulate cortices (7). Visual assessment of 18F-AZD4694 PET scans were defined by the consensus of two neurologists blinded to clinical diagnosis as described in (27). Briefly, images were rated as positive if cortical binding exceeded white matter binding in more than one region.

Statistical analyses

Baseline demographics were assessed using multiple t tests and χ^2 tests using the R Statistical Software Package version 3.3 (<http://www.r-project.org/>). We used five analytical methods to derive a quantitative cut-off for 18F-AZD4694 SUVR: (i) two standard deviations above the mean of a reference group of cognitively unimpaired young adults (7,28) (ii) Area under the Receiver Operating Characteristic (ROC) curve comparing CU elderly and AD dementia subjects (29) (iii) Area under the ROC curve comparing visually amyloid-negative and visually

amyloid positive scans (iv) Gaussian Mixture Modeling (30) and (v) Area under the ROC curve comparisons with CSF measurements of amyloid- β (31). Because existing evidence does not support sex differences between males and females in amyloid-PET uptake (32), we did not correct analyses for sex such that a single threshold of abnormality could be applied to both sexes. Similarly, in line with the NIA-AA research framework, we chose to determine a single threshold for amyloid-PET positivity and not one that differs according to a subject's age. Higher thresholds in older individuals could result in falsely identifying these individuals as negative.

For ROC analyses, we determined sensitivity and specificity for various cut-offs and optimal threshold. The optimal threshold value was calculated using the least distance from a point to the ROC curve (0,1; best operating point) contrasting AD dementia vs CU elderly groups, visually positive vs visually negative groups and CSF-negative vs CSF-positive groups. This provides the best trade-off between sensitivity and specificity for differentiating between two dichotomous categories. We chose to contrast visually positive vs visually negative cases in addition to CU elderly vs AD dementia for two reasons: (i) post-mortem evaluations consistently show CU elderly individuals frequently present with elevated amyloid- β pathology at levels that are indistinguishable from individuals with AD dementia (33,34) and (ii) a substantial portion of clinically diagnosed AD dementia individuals do not display amyloid- β pathology upon post-mortem evaluation (35). Thus, defining cut-points based on individuals who do or do not meet specific clinical criteria bears conceptual limitations (7). Concordance with visual reads has also been used for threshold validation of other fluorinated amyloid-PET radioligands (36).

RESULTS

Demographic and clinical information is summarized in Table 1. We observed significant differences in amyloid-PET ligand uptake across groups, with CI individuals showing the highest, followed by CU elderly, with young individuals presenting with low amyloid- β ligand uptake. We observed a similar pattern with CSF measures of $A\beta_{42}/A\beta_{40}$ ratios. CI individuals were more likely to be *APOE* $\epsilon 4$ carriers. Fig. 1 displays four ^{18}F -AZD4694 PET scans, representing the range of ^{18}F -AZD4694 SUVR: one young adult, a CU elderly amyloid- β negative, CU elderly amyloid- β positive and an amyloid- β positive AD dementia individual. In our sample, 0% of young individuals, 29% of CU elderly and 72% of CI individuals were deemed ^{18}F -AZD4694 PET positive based on visual assessment.

Means and standard deviations from the CU young adults ($n=22$) compared to CU elderly and CI groups are displayed in Fig. 2. CU young individuals displayed low ^{18}F -AZD4694 PET uptake (mean=1.14) as well as low SDs ($SD=0.09$). The mean + 2SD of ^{18}F -AZD4694 PET SUVR from the CU young individual group was 1.33, displayed as the dashed line in Fig. 2 (PVC data presented in Supplemental Fig. 2).

Fig. 3 displays ROC curves used to determine the quantitative threshold that best agreed with clinical diagnosis (top row) and that best agreed with visual assessment from trained raters (bottom row). When contrasting CU elderly with AD dementia groups, we observed a good area under the curve ($AUC=82.5\%$, sensitivity=85%, specificity=73%). The optimal threshold at this point was 1.56 SUVR, represented by the dashed line. When contrasting visually $A\beta^+$ vs $A\beta^-$ groups, we observed an excellent area under the curve ($AUC=97\%$, sensitivity=91%,

specificity=95%). The optimal threshold at this point was 1.55 SUVR. These thresholds were similar when using PVC data (Supplemental Fig. 3). When contrasting only visually A β - CU elderly vs visually A β + AD dementia individuals, the optimal threshold was 1.58 SUVR (Supplemental Fig. 4).

When employing Gaussian Mixture Modeling, we derived two components, one corresponding to low amyloid- β individuals (mean=1.28, SD=0.136) and one to high amyloid- β individuals (mean=2.19, SD=0.45) (Fig. 4). The optimal cut off point from Gaussian Mixture Modeling was 1.55 SUVR. Gaussian Mixture Modeling using PVC data gave similar results (Supplemental Fig. 5). When including the CU young adults in the Gaussian Mixture Modeling analysis, we observed a similar threshold of 1.54 SUVR (Supplemental Fig. 6).

We assessed correspondence between CSF amyloid positivity based on a A β ₄₂/A β ₄₀ ratio of 0.068 (Fig. 5). The optimal 18F-AZD4694 threshold was 1.51, represented by the dashed line (area under the ROC curve=95%, sensitivity=88.9%, specificity=91.4%). This threshold was similar when employing PVC data (Supplemental Fig. 7). Supplementary Table 1 summarizes the thresholds obtained from all methods, along with the percentage of the CU elderly population that would be labeled amyloid- β positive according to each method.

DISCUSSION

In this study, we present evidence from converging analytical and biomarker techniques for an 18F-AZD4694 PET threshold for amyloid- β positivity. We observed convergent results

from CSF measurements of amyloid positivity, Gaussian Mixture Modeling and ROC curve analyses, all pointing to an optimal value of 1.55 SUVR.

All methods to dichotomize continuous measures invariably lead to a number of conceptual and analytical idiosyncrasies with respect to the threshold for classification. To help address this issue, we employed multiple analytical methods as well as validation with CSF measurements of amyloid- β . The first of these methods, using the mean +2 SD of cognitively unimpaired young adults, resulted in a 18F-AZD4694 SUVR threshold of 1.33. Using this threshold, over 50% of our CU elderly population would be amyloid- β positive, which does not agree with observations from post-mortem studies of amyloid- β pathology (33). Other groups applying the mean +2 SD method using [^{11}C]PiB have also found it to be unsuitable (7), potentially due to age-related nonspecific uptake (37). When using ROC curves contrasting CU elderly with AD dementia groups, we observed an optimal threshold of 1.56 SUVR. When using ROC curves contrasting visually negative vs visually positive cases, we observed an optimal threshold of 1.55 SUVR. Gaussian Mixture Modeling produced an identical threshold of 1.55 SUVR separating low 18F-AZD4694 from high 18F-AZD4694 groups. Finally, the threshold derived from CSF (1.51) was slightly lower than the ROC and gaussian mixture modeling methods using PET data, possibly reflecting CSF amyloid- β becoming abnormal before amyloid-PET (38). Taken together, we chose a cut-off of 1.55 SUVR for three reasons: (i) because the goal of this study is to define a quantitative threshold for amyloid-PET positivity (in contrast to CSF positivity) (ii) because of the agreement between both ROC and Gaussian Mixture Modeling methods and (iii) because longitudinal studies indicate that patients who are CSF+/PET- have a better prognosis over 5 years as compared to

CSF+/PET+ patients, indicating amyloid-PET positivity has greater specificity for AD-related cognitive decline and biomarker changes (39).

While a cut-off of 1.55 SUVR is higher than published cut-offs for other fluorinated amyloid-PET radioligands, it is important to consider that 18F-AZD4694 displays a higher B_{\max}/K_d (concentration of available binding sites / equilibrium dissociation constant) ratio than other fluorinated amyloid-PET radioligands (16). Furthermore, while 18F-AZD4694 is structurally similar to [^{11}C]PiB (18) and has a similar K_d ([^{11}C]PiB $K_d = 1\text{-}2\text{ nM}$ (40)), 18F-AZD4694's longer scanning time and longer radioactive half-life result in higher counts, likely underlying the slightly higher SUVR threshold for positivity reported in our study compared to [^{11}C]PiB thresholds (7,41). This is consistent with head-to-head studies between [^{11}C]PiB and 18F-AZD4694 providing evidence that 18F-AZD4694 has a slightly larger effect size difference in binding between CU and AD individuals (18).

Visual reads of amyloid-PET scans are most commonly employed in clinical settings (9) to help account for differences in PET acquisition protocols, processing methods, or binding properties of individual radioligands. Limitations of visual ratings include in-rater reliability, need for expert raters, lack of standardization for rating methods across radiotracers (14). While quantitative measurements have their utility in research settings, they may also be clinically helpful in resolving cases of discordance between raters, helping centers with less expertise (14), or situations when a scan appears "borderline" (42). Furthermore, with potential disease-modifying therapies on the horizon, the need for quantitative or semi-quantitative measurements of amyloid- β load during follow-up of patients treated in a clinical environment will clearly be present.

In vivo semi-quantification of amyloid- β pathology using PET has enabled a multitude of new possibilities for the field of AD, including establishing core biomarker models (4,5) and guiding clinical trial design (10). While most research has focused on dichotomous classification of amyloid-PET imaging into positive and negative groups, the spatial resolution of PET provides the opportunity for staging of amyloid-PET (43). Staging systems may provide additional information by leveraging the topographical distribution of amyloid-PET uptake, which may aid in the patient monitoring during the course of AD. While our study was not designed to assess regional patterns of amyloid- β accumulation, region-specific approaches may have increased sensitivity as compared to global measures, provided they are replicable.

It is important to consider that the Translational Biomarkers in Aging and Dementia cohort constitutes a sample with a significantly higher proportion of AD and MCI individuals than found in the general population. Furthermore, like several longitudinal prospective cohort studies, our study is enriched for *APOE ϵ 4* carriers (44), who are at risk of becoming amyloid positive before *APOE ϵ 4* noncarriers. Finally, all 18F-AZD4694 PET scans in this study are acquired on a brain-dedicated HRRT PET camera. Thus, the threshold from our sample may potentially differ from other prospective longitudinal cohort studies of aging and dementia. Correspondingly, the threshold of 1.55 SUVR is not intended to be a threshold applied in other centers without validation with respect to local PET acquisition and processing methods.

Our results should be considered in the context of several limitations. Because at this time point we do not have access to a large database of longitudinal 18F-AZD4694 PET data, we were

not able to make calculations based on the “reliable worsening” method, the value at which that biomarker reliably changes (7). A second limitation is the use of static scans with SUVR as an outcome measure: this introduces potential limitations due to individual differences in tracer brain delivery and washout compared to dynamic PET and BP_{nd} as an outcome measure (45) though kinetic analyses of other fluorinated amyloid-PET ligands report that these effects are small (46). Recent studies using have also reported that SUVR overestimates true 18F-Florbetapir binding (47). It is also important to consider that SUVR maps result in more discordant case reads when used by experienced observers as compared to BP_{nd} maps (15). Third, a large autopsy series is not available in our cohort, which precludes comparing our threshold with gold standard autopsy methods. To the best of our knowledge, existing ex-vivo studies with 18F-AZD4694 are restricted to autoradiographic evaluations of this radiotracer (16). Future case-to-autopsy studies are needed to determine the degree of correspondence between 18F-AZD4694 PET positivity and neuropathological criteria. Finally, future studies are needed to validate the associations between 18F-AZD4694 PET positivity and longitudinal cognitive decline.

CONCLUSION

In conclusion, we provide convergent evidence from multiple analytical methods pointing to an 18F-AZD4694 SUVR threshold of 1.55 for determining amyloid- β positivity. Given the increasing use of dichotomized amyloid-PET results in clinical care (8,9), a quantitative threshold may provide clinicians with additional information to help in discordant or borderline cases.

DISCLOSURE

No conflicts of interest relevant to this article exist.

ACKNOWLEDGEMENTS

JT is funded by McGill University's Faculty of Medicine Scholarship. This work is supported by the Canadian Institutes of Health Research (CIHR) (MOP-11-51-3), the Alzheimer's Association (NIRG-12- 92090, NIRP-12-259245), Fonds de Recherche du Québec–Santé (Chercheur Boursier and 2020-VICO-279314). HZ is a Wallenberg Scholar supported by grants from the Swedish Research Council (#2018-02532), the European Research Council (#681712), Swedish State Support for Clinical Research (#ALFGBG-720931), the Alzheimer Drug Discovery Foundation (ADDF), USA (#201809-2016862), and the UK Dementia Research Institute at UCL.KB is supported by the Swedish Research Council (#2017-00915), the Alzheimer Drug Discovery Foundation (ADDF), USA (#RDAPB-201809-2016615), the Swedish Alzheimer Foundation (#AF-742881), Hjärnfonden, Sweden (#FO2017-0243), the Swedish state under the agreement between the Swedish government and the County Councils, the ALF-agreement (#ALFGBG-715986), and European Union Joint Program for Neurodegenerative Disorders (JPND2019-466-236).

KEY POINTS:

QUESTION: What is the quantitative threshold for determining amyloid positivity using the high-affinity radioligand 18F-AZD4694?

PERTINENT FINDINGS: We observed converging evidence from multiple analytical methods that an 18F-AZD4694 threshold of 1.55 SUVR is the optimal threshold for determining amyloid-positivity.

IMPLICATIONS FOR PATIENT CARE: With the use of amyloid-PET in clinical contexts approaching, quantitative thresholds may be helpful for arbitrating disagreement among raters or classifying borderline cases.

REFERENCES

1. Klunk WE, Engler H, Nordberg A, et al. Imaging Brain Amyloid in Alzheimer's Disease with Pittsburgh Compound-B. *Ann Neurol.* 2004;55:306-319.
2. Blennow K, Zetterberg H. Biomarkers for Alzheimer's disease: current status and prospects for the future. *J Intern Med.* 2018;6:643-663.
3. Shaw LM, Arias J, Blennow K, et al. Appropriate use criteria for lumbar puncture and cerebrospinal fluid testing in the diagnosis of Alzheimer's disease. *Alzheimer's Dement.* 2018;14:1505-1521.
4. Bateman RJ, Xiong C, Benzinger TLS, et al. Clinical and Biomarker Changes in Dominantly Inherited Alzheimer's Disease. *N Engl J Med.* 2012;367:795-804.
5. Jack CR, Knopman DS, Jagust WJ, et al. Tracking pathophysiological processes in Alzheimer's disease: An updated hypothetical model of dynamic biomarkers. *Lancet Neurol.* 2013;12:207-216.
6. Jack CR, Bennett DA, Blennow K, et al. NIA-AA Research Framework: Toward a biological definition of Alzheimer's disease. *Alzheimer's Dement.* 2018;14:535-562.
7. Jack CR, Wiste HJ, Weigand SD, et al. Defining imaging biomarker cut points for brain aging and Alzheimer's disease. *Alzheimer's Dement.* 2017;13:205-216.
8. Johnson KA, Minoshima S, Bohnen NI, et al. Appropriate use criteria for amyloid PET: a report of the Amyloid Imaging Task Force, the Society of Nuclear Medicine and Molecular Imaging, and the Alzheimer's Association. *Alzheimers Dement.* 2013;54:476-490.
9. Rabinovici GD, Gatsonis C, Apgar C, et al. Association of Amyloid Positron Emission

- Tomography with Subsequent Change in Clinical Management among Medicare Beneficiaries with Mild Cognitive Impairment or Dementia. *JAMA*. 2019;321:1286-1294.
10. Sperling RA, Rentz DM, Johnson KA, et al. The A4 Study: Stopping AD Before Symptoms Begin? *Sci Transl Med*. 2014;6:228fs13-228fs13.
 11. Sevigny J, Chiao P, Bussière T, et al. The antibody aducanumab reduces A β plaques in Alzheimer's disease. *Nature*. 2016;537:50-56.
 12. Chiao P, Bedell BJ, Avants B, et al. Impact of reference and target region selection on amyloid PET SUV ratios in the phase 1B PRIME study of aducanumab. *J Nucl Med*. 2019;60:106-109.
 13. Clark CM, Schneider JA, Bedell BJ, et al. Use of florbetapir-PET for imaging β -amyloid pathology. *JAMA*. 2011;305:275-283.
 14. Bischof G, Bartenstein P, Barthel H, et al. Comparing Amyloid PET Tracers and Interpretation Strategies: First Results from the CAPTAINs Study. *J Nucl Med*. 2018;59:485.
 15. Collij LE, Konijnenberg E, Reimand J, et al. Assessing amyloid pathology in cognitively normal subjects using 18F-flutemetamol PET: Comparing visual reads and quantitative methods. *J Nucl Med*. 2019;60:541-547.
 16. Juréus A, Swahn BM, Sandell J, et al. Characterization of AZD4694, a novel fluorinated A β plaque neuroimaging PET radioligand. *J Neurochem*. 2010;114:784-794.
 17. Villemagne VL, Rowe CC. Amyloid PET ligands for dementia. *PET Clin*. 2010;5:33-53.
 18. Rowe CC, Pejoska S, Mulligan RS, et al. Head-to-Head Comparison of 11C-PiB and 18F-AZD4694 (NAV4694) for β -Amyloid Imaging in Aging and Dementia. *J Nucl Med*. 2013;54:880-886.

19. Therriault J, Benedet AL, Pascoal TA, et al. Association of Apolipoprotein e ϵ 4 with Medial Temporal Tau Independent of Amyloid- β . *JAMA Neurol.* 2020;77:470-479.
20. Jack CR, Wiste HJ, Botha H, et al. The bivariate distribution of amyloid- β and tau: relationship with established neurocognitive clinical syndromes. *Brain.* 2019;142:3230-3242.
21. Petersen RC. Mild cognitive impairment as a diagnostic entity. In: *Journal of Internal Medicine.* Vol 256. ; 2004:183-194.
22. McKhann GM, Knopman DS, Chertkow H, et al. The diagnosis of dementia due to Alzheimer's disease: Recommendations from the National Institute on Aging-Alzheimer's Association workgroups on diagnostic guidelines for Alzheimer's disease. *Alzheimer's Dement.* 2011;7:263-269.
23. Leitão MJ, Silva-Spínola A, Santana I, et al. Clinical validation of the Lumipulse G cerebrospinal fluid assays for routine diagnosis of Alzheimer's disease. *Alzheimer's Res Ther.* 2019;11:1-12.
24. Hansson O, Lehmann S, Otto M, Zetterberg H, Lewczuk P. Advantages and disadvantages of the use of the CSF Amyloid β (A β) 42/40 ratio in the diagnosis of Alzheimer's Disease. *Alzheimer's Res Ther.* 2019;11:1-15.
25. Lewczuk P, Matzen A, Blennow K, et al. Cerebrospinal Fluid A β 42/40 Corresponds Better than A β 42 to Amyloid PET in Alzheimer's Disease. *J Alzheimer's Dis.* 2017.
26. Fonov V, Coupé P, Eskildsen S, et al. Atrophy specific MRI brain template for Alzheimer's disease and Mild Cognitive Impairment. *Alzheimer's Dement.* 2011;7:S58.
27. Ng KP, Therriault J, Kang MS, et al. Rasagiline, a monoamine oxidase B inhibitor, reduces in vivo [18F]THK5351 uptake in progressive supranuclear palsy. *NeuroImage*

- Clin.* 2019;24:102091.
28. Villeneuve S, Rabinovici GD, Cohn-Sheehy BI, et al. Existing Pittsburgh Compound-B positron emission tomography thresholds are too high: Statistical and pathological evaluation. *Brain.* 2015;138:2020-2033.
 29. Landau SM, Breault C, Joshi AD, et al. Amyloid- β Imaging with Pittsburgh Compound B and Florbetapir: Comparing Radiotracers and Quantification Methods and Initiative for the Alzheimer's Disease Neuroimaging. *Soc Nucl Med.* 2013;54:70-77.
 30. Bertens D, Tijms BM, Scheltens P, Teunissen CE, Visser PJ. Unbiased estimates of cerebrospinal fluid β -amyloid 1-42 cutoffs in a large memory clinic population. *Alzheimer's Res Ther.* 2017;9:1-8.
 31. Landau SM, Lu M, Joshi AD, et al. Comparing positron emission tomography imaging and cerebrospinal fluid measurements of β -amyloid. *Ann Neurol.* 2013;74:826-836.
 32. Sperling RA, Donohue MC, Raman R, et al. Association of Factors With Elevated Amyloid Burden in Clinically Normal Older Individuals. *JAMA Neurol.* 2020;(in press):1-11.
 33. Knopman DS, Parisi JE, Salviati A, et al. Neuropathology of Cognitively Normal Elderly. *J Neuropathol Exp Neurol.* 2003;62:1087-1095.
 34. Schmitt FA, Davis DG, Wekstein DR, Smith CD, Ashford JW, Markesbery WR. "Preclinical" AD revisited: Neuropathology of cognitively normal older adults. *Neurology.* 2000;55:370-376.
 35. Knopman DS, Petersen RC, Jack CR. A brief history of "Alzheimer disease": Multiple meanings separated by a common name. *Neurology.* 2019;92:1053-1059.
 36. Thurfjell L, Lilja J, Lundqvist R, et al. Automated quantification of 18F-flutemetamol

- PET activity for categorizing scans as negative or positive for brain amyloid: Concordance with visual image reads. *J Nucl Med.* 2014;55:1623-1628.
37. Lowe VJ, Lundt ES, Senjem ML, et al. White matter reference region in PET studies of ¹¹C-Pittsburgh compound B uptake: Effects of age and amyloid- β deposition. *J Nucl Med.* 2018;59:1583-1589.
 38. Mattsson N, Insel PS, Donohue M, et al. Independent information from cerebrospinal fluid amyloid- β and florbetapir imaging in Alzheimer's disease. *Brain.* 2015;138:772-783.
 39. Reimand J, Collij L, Scheltens P, Femke Bouwman ;, Ossenkuppele R. Amyloid- β CSF/PET discordance vs tau load 5 years later: It takes two to tangle. 2020.
 40. Mathis CA, Wang Y, Holt DP, Huang GF, Debnath ML, Klunk WE. Synthesis and evaluation of ¹¹C-labeled 6-substituted 2-arylbenzothiazoles as amyloid imaging agents. *J Med Chem.* 2003;46:2740-2754.
 41. Villemagne VL, Burnham S, Bourgeat P, et al. Amyloid-B deposition, neurodegeneration, and cognitive decline in sporadic Alzheimer's disease: A prospective cohort study. *Lancet Neurol.* 2013;12:357-367.
 42. Mormino EC, Brandel MG, Madison CM, et al. Not quite PIB-positive, not quite PIB-negative: Slight PIB elevations in elderly normal control subjects are biologically relevant. *Neuroimage.* 2012;59:1152-1160.
 43. Fantoni E, Collij L, Alves IL, Buckley C, Farrar G. The Spatial-Temporal Ordering of Amyloid Pathology and Opportunities for PET Imaging. *J Nucl Med.* 2020;61:166-171.
 44. Therriault J, Benedet AL, Pascoal TA, et al. APOE ϵ 4 potentiates the relationship between amyloid- β and tau pathologies. *Mol Psychiatry.* 2020:epub ahead of print.
 45. Boellaard R. Standards for PET Image Acquisition and Quantitative Data Analysis. *J Nucl*

Med. 2009;50:11S--20S.

46. Bullich S, Barthel H, Koglin N, et al. Validation of noninvasive tracer kinetic analysis of ¹⁸F-Florbetaben PET using a dual-time-window acquisition protocol. *J Nucl Med.* 2018;59:1104-1110.
47. Golla SSV, Verfaillie SCJ, Boellaard R, et al. Quantification of [¹⁸F]florbetapir: A test–retest tracer kinetic modelling study. *J Cereb Blood Flow Metab.* 2019;39:2172-2180.

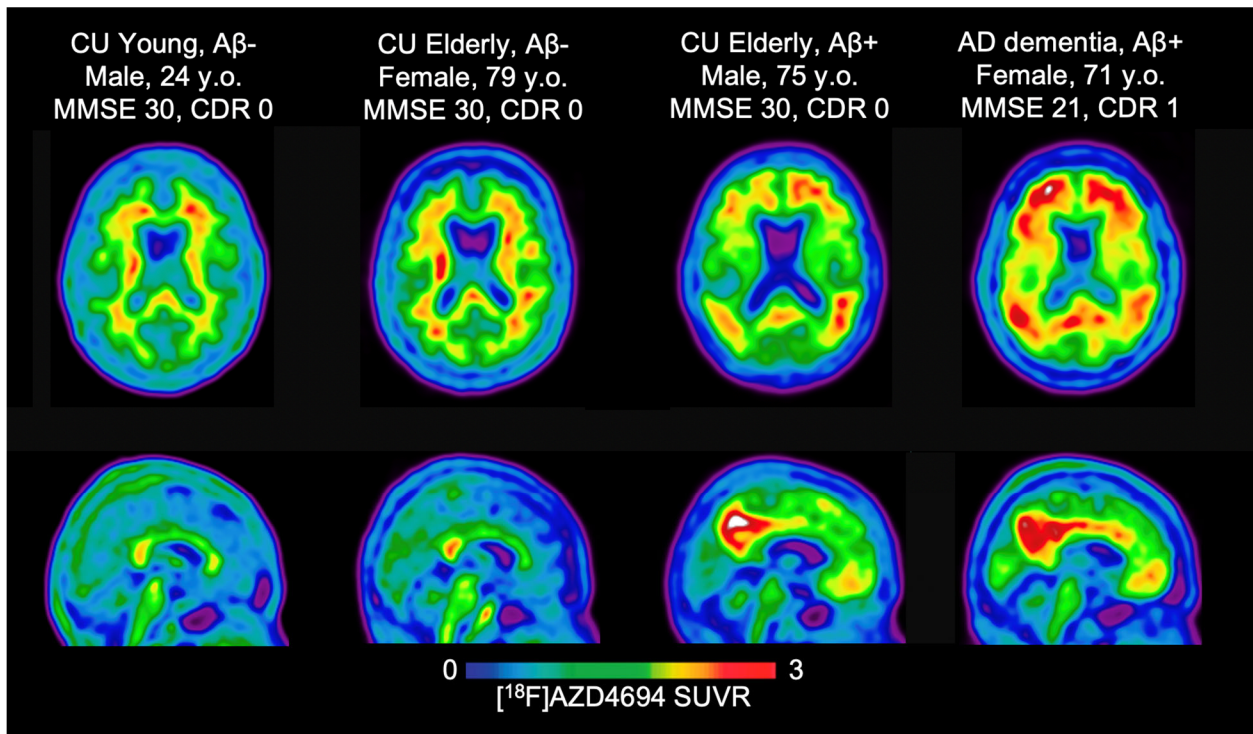


Figure 1: Representative images of AZD4694 SUVR PET images.

Transaxial (top) and midsagittal (bottom) ^{18}F -AZD4694 PET images of four subjects representing the range of binding patterns in the present study. All images are presented in template space. MNI coordinates: $x=2$, $y = -59$, $z = 15$

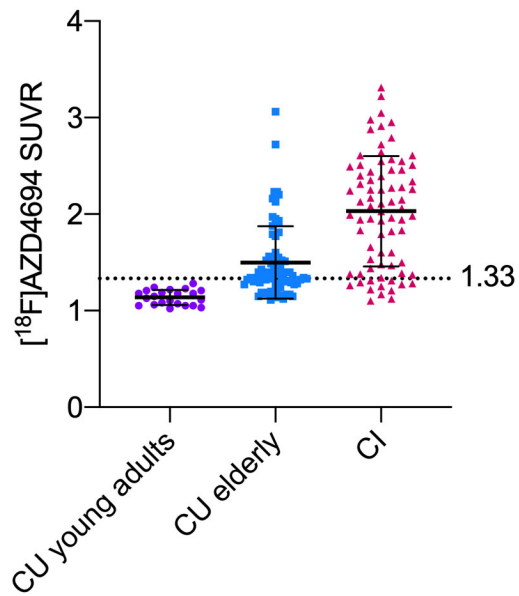


Figure 2: ^{18}F -AZD4694 PET in all groups.

Means and standard deviations of cognitively unimpaired young adults (age < 25 years), cognitively unimpaired elderly and cognitively impaired groups. Error bars (in black) correspond to each group's mean and standard deviation in ^{18}F -AZD4694 SUVR. Young adults displayed minimal amyloid PET uptake (mean = 1.14, SD = 0.09). The dashed line represents two standard deviations above the mean of young adults, at 1.33 ^{18}F -AZD4694 SUVR.

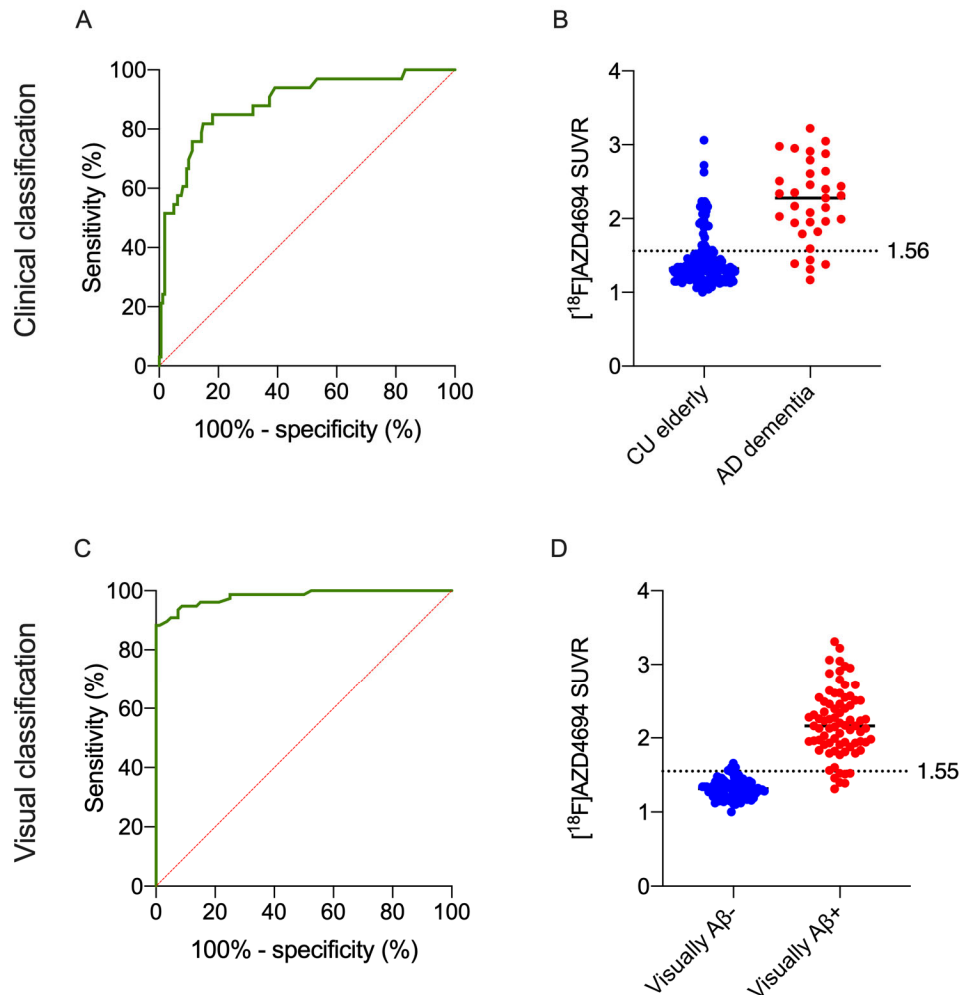


Figure 3: ROC Curve contrasting visually positive vs visually negative cases.

Top row: When contrasting CU elderly with AD dementia groups, we observed a good area under the curve (AUC = 82.5%, sensitivity 85%, specificity 73%). B: The optimal threshold at this point was 1.56 SUVR, represented by the dashed line. Bottom row: C: The Area under the ROC curve contrasting visually negative vs visually positive cases displayed an excellent AUC (AUC=97%, sensitivity: 90.91%, specificity: 95%). D: ^{18}F -AZD4694 PET means for visually positive (red) and visually negative (blue) groups. The dashed line represents the optimal threshold derived from the ROC curve (1.55 SUVR).

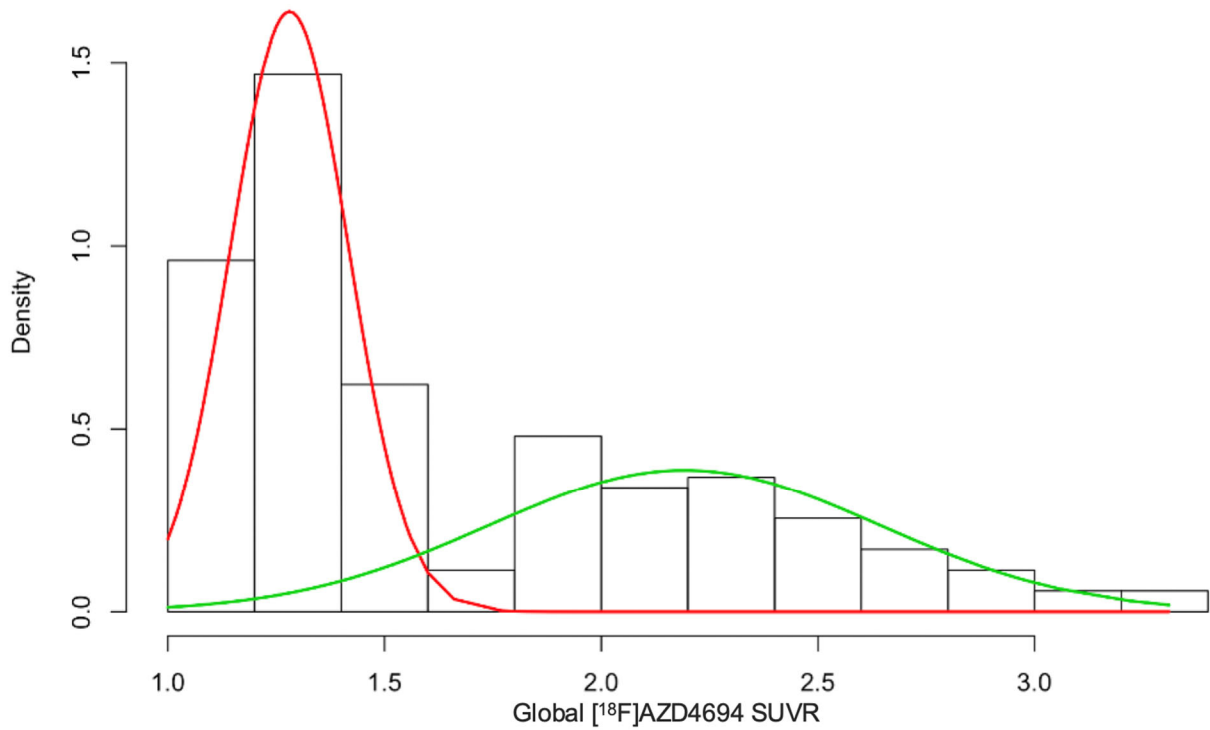


Figure 4: Gaussian Mixture Modeling

Gaussian mixture modeling representing two distributions. Low ^{18}F -AZD4694 (red) and high (green) ^{18}F -AZD4694 gaussian distributions are superimposed on the subject density histogram for all ^{18}F -AZD4694 PET SUVRs from the CU elderly and CI populations. The optimal cut point from Gaussian mixture modeling was 1.55 SUVR.

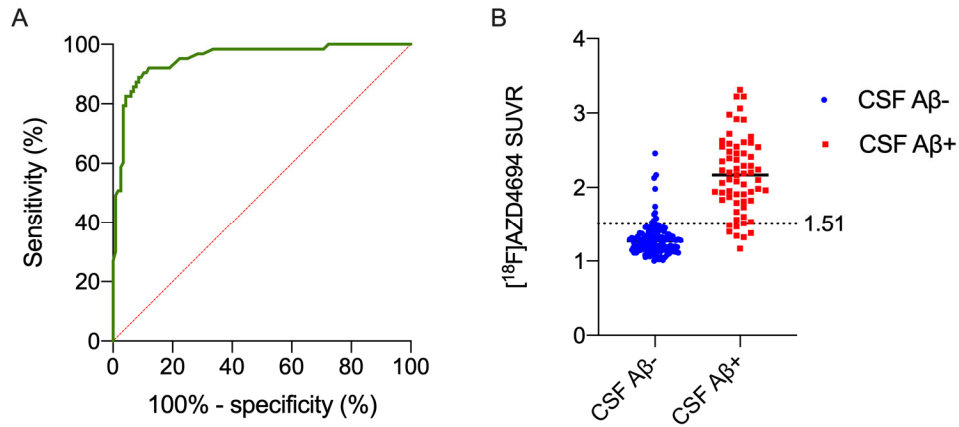


Figure 5: ROC Curve contrasting CSF positive vs negative individuals.

A: The Area under the ROC curve contrasting individuals dichotomized on the basis of their cerebrospinal measure of $A\beta_{42}/A\beta_{40}$ ratio. This method resulted in an area under the ROC curve of (AUC=95%, sensitivity=88.9%, specificity=91.4%). B: AZD4694 PET means for CSF negative (blue) and CSF positive (red). The dashed line represents the optimal threshold derived from the ROC curve (1.51 SUVR).

Table 1. Demographic, clinical and biomarker characteristics of the sample.

| | CU Young | CU Elderly | CI | <i>p</i> value CU Young vs CU Elderly | <i>p</i> value CU Elderly vs CI |
|---|--------------|--------------|--------------|--|------------------------------------|
| No. | 22 | 89 | 65 | - | - |
| Age, y, mean (SD) | 22.7 (1.3) | 72.33 (5.88) | 67.91 (8.97) | <0.0001 | 0.0004 |
| Female, no. (%) | 14 (63) | 51 (57) | 36 (55) | 0.59 | 0.81 |
| Education, y, mean (SD) | 16.61 (1.33) | 15.06 (3.81) | 15.1 (3.34) | 0.06 | 0.94 |
| <i>APOE</i> ε4 carriers, % | 6 (27) | 33 (37) | 41 (63) | 0.58 | <0.0001 |
| MMSE, mean (SD) | 29.77 (0.53) | 29.12 (1.07) | 24.03 (6.07) | 0.009 | <0.0001 |
| Neocortical 18F-AZD4694 SUVR (SD) | 1.14 (0.09) | 1.48 (0.38) | 2.04 (0.57) | <0.0001 | <0.0001 |
| CSF Aβ ₄₂ /Aβ ₄₀ (SD) | 0.09 (0.006) | 0.07 (0.02) | 0.05 (0.02) | <0.0001 | <0.0001 |

Mean and standard deviation (SD) are provided for continuous variables; number and % are provided for dichotomous variables. *P* values indicate values assessed with two-sided independent samples t-tests for each variable except sex and *APOE* ε4 status, where contingency chi-square tests were performed. CU = Cognitively Unimpaired; CI = Cognitively Impaired; CSF: Cerebrospinal Fluid; MMSE = Mini-Mental State Examination; SUVR = Standardized Uptake Value Ratio.

Radiosynthesis of ^{18}F -AZD4694

The ^{18}F -AZD4694 was synthesized using the following procedure. No-carrier-added (nca) aqueous ^{18}F -fluoride prepared by the $^{18}\text{O}(\text{p},\text{n})^{18}\text{F}$ nuclear reaction on an enriched [^{18}O] water (98%) target was passed through a preconditioned (10mL 0.05M K_2CO_3 , 10mL deionized water) Sep Pak Light QMA cartridge (Waters). The ^{18}F -fluoride is then eluted off the QMA cartridge and into the reactor with a solution of 1.5 mL acetonitrile containing 11 ± 1 mg Kryptofix 2.2.2. and 15-20 μmol potassium carbonate. The solution is then evaporated to dryness repeatedly with additional acetonitrile at a temperature of 95 $^\circ\text{C}$, a stream of inert gas and reduced pressure. After 15 min, a solution of 3 mg of precursor (AZD4694) in 1 mL DMSO is added to the reactor, and is heated to 105 $^\circ\text{C}$ for 7 min. During this step, the product ^{18}F -NAV4694 in its protected form is generated (Supplemental Fig. 1).

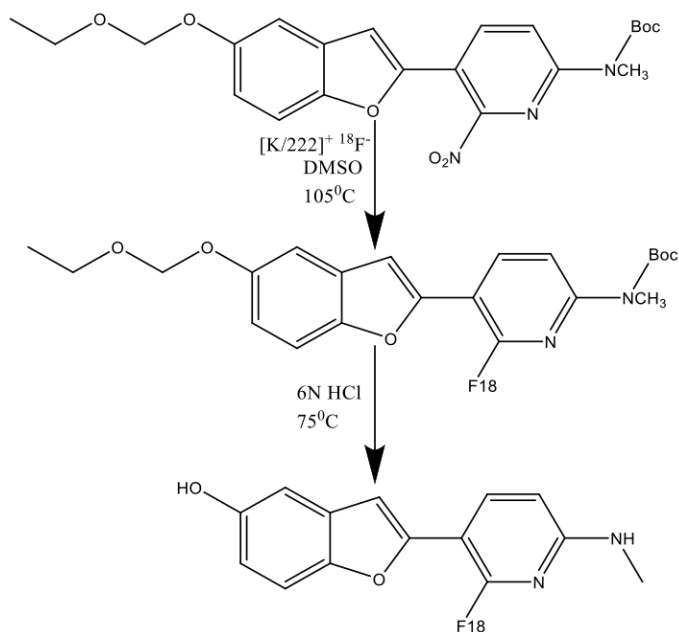
The reactor is then cooled to 75 $^\circ\text{C}$, and 0.5 mL 6N HCl is added, and heated to 75 $^\circ\text{C}$ for 5 min for deprotection. Then 0.5 mL 5N sodium hydroxide solution and 0.5 mL HPLC solvent (20 mM ammonium formate/methanol; 40/60) is added. The resulting mixture is transferred into an injector loop of the HPLC system and is purified on a Phenomenex Luna 10 μ C-18 column, with a flow of 3 mL/min. The desired product elutes at a retention time of 24-28 min. Impurities as well as radioactive impurities and unreacted fluoride elute at earlier retention times, and are thus transferred into the waste container. The product peak is collected into a vial containing 15ml of water and 25 μl ascorbic acid. The solution is passed through a C18 cartridge. The cartridge is washed with an additional 10ml of water. The product is eluted from the cartridge into a sterile vial with 0.5ml of ethanol followed by 9.5ml of sterile phosphate buffer and 25 μl of ascorbic acid.

Supplementary Table 1: Optimal cut-offs for 18F-AZD4694 PET positivity

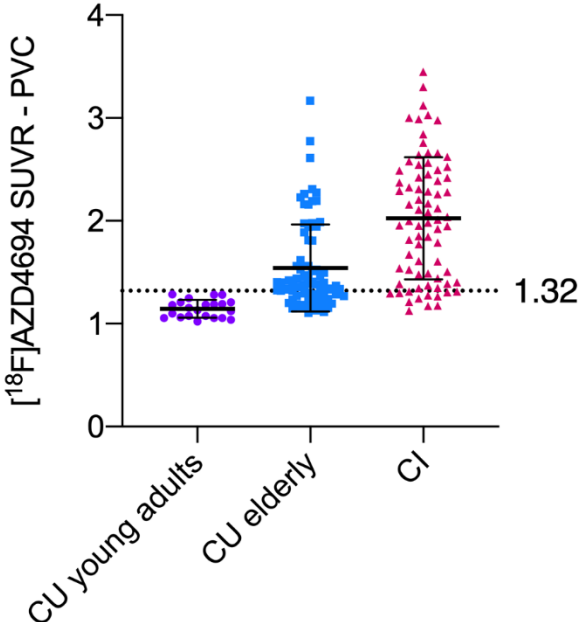
| | 2 SD above mean of young controls | CSF A β ₄₂ /A β ₄₀ positivity | ROC curve contrasting AD dementia and CU elderly | ROC curve contrasting visual ratings | Gaussian Mixture Modeling |
|---|-----------------------------------|---|--|--------------------------------------|---------------------------|
| 18F-AZD4694 SUVR threshold | 1.33 | 1.51 | 1.56 | 1.55 | 1.55 |
| % of CU elderly A β positive according to threshold | 52% | 29% | 25% | 26% | 26% |

This table summarizes the SUVR cut-point derived from each of the five methods assessed in this study, along with the corresponding percentage of the CU elderly population that would be labeled as positive according to each method. A β : amyloid- β ; AD: Alzheimer's disease; CSF: Cerebrospinal Fluid; CU: Cognitively unimpaired; ROC: Receive Operating Characteristic; SD: Standard deviation; SUVR: Standardized Uptake Value Ratio.

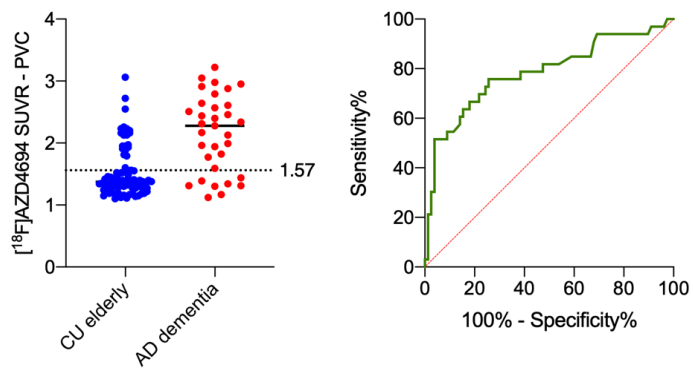
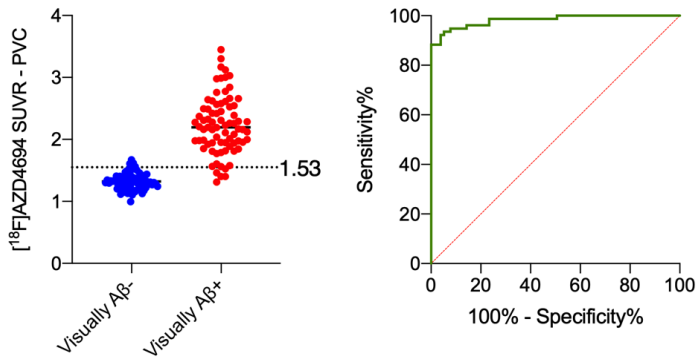
Supplemental Fig. 1



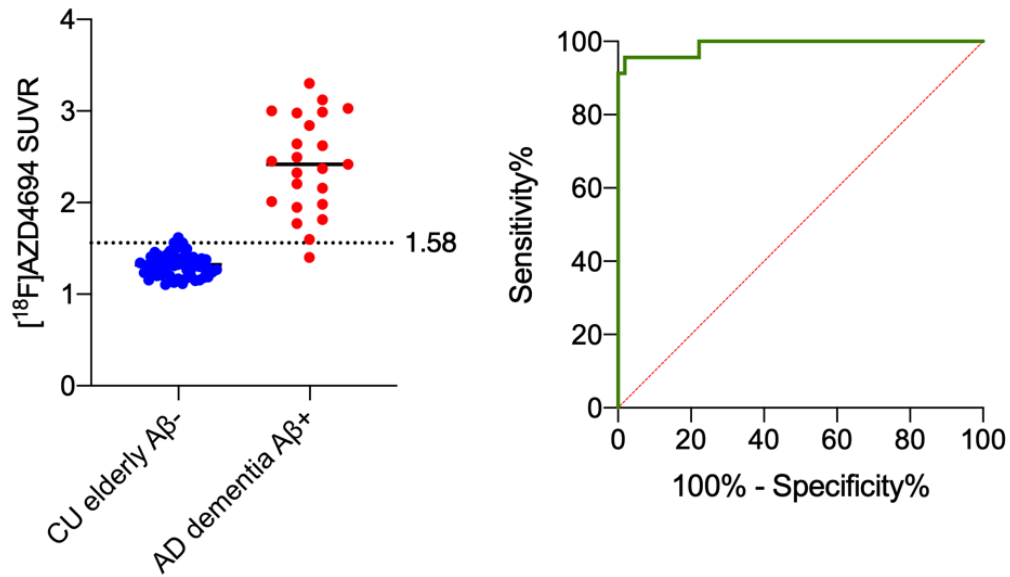
Supplemental Fig. 2



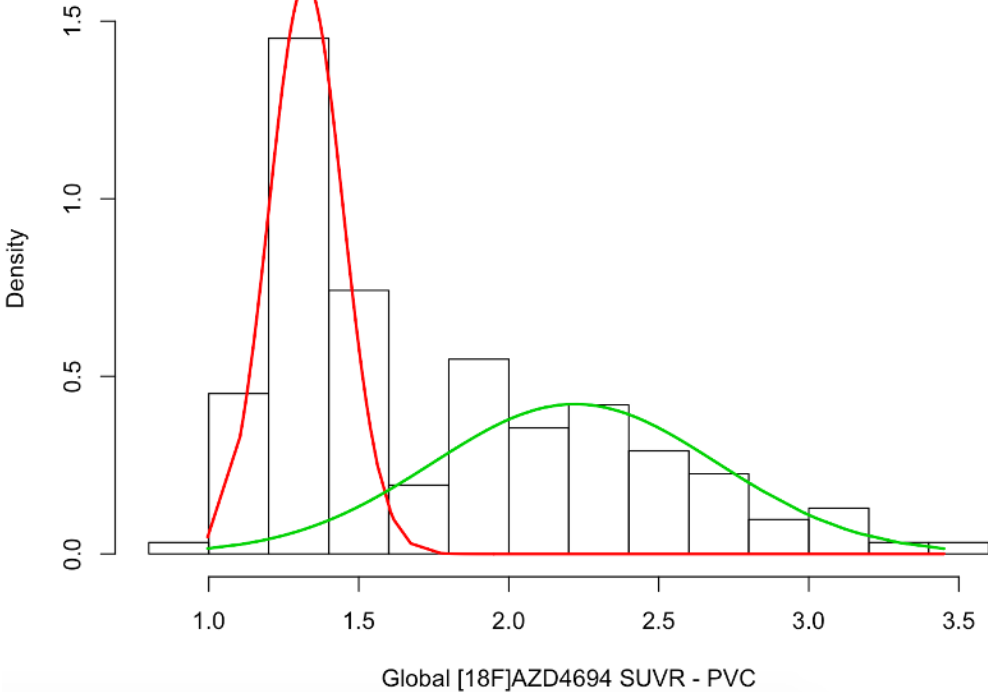
Supplemental Fig. 3



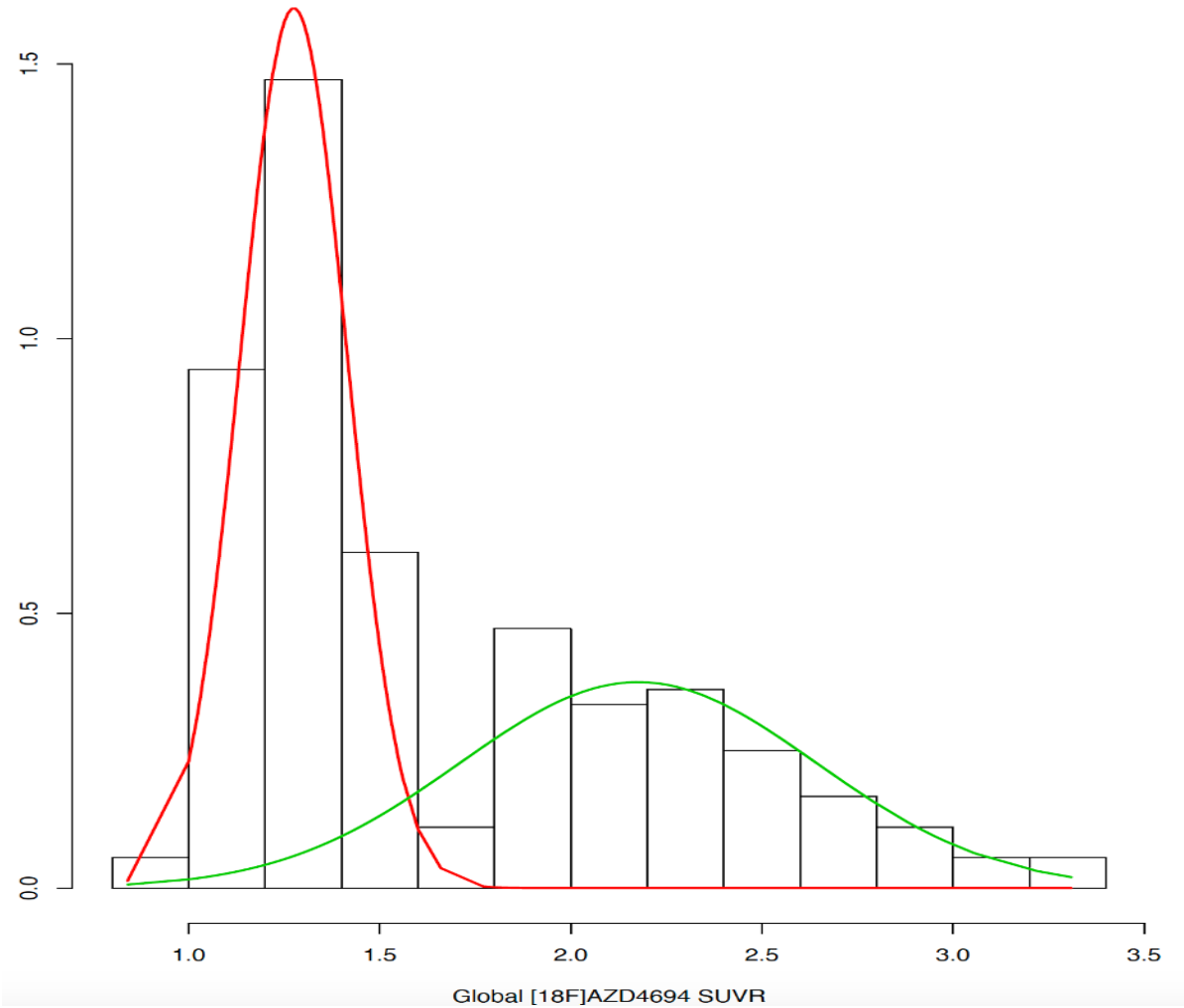
Supplemental Fig. 4



Supplemental Fig. 5



Supplemental Fig. 6



Supplemental Fig. 7

